Inorganic Chemistry

Article

pubs.acs.org/IC

Pressure-Dependent Reversible Increase in T_c for the Ferrimagnetic 2-D $Mn^{II}(TCNE)I(OH_2)$ and 3-D $Mn^{II}(TCNE)_{3/2}(I_3)_{1/2}\cdot zTHF$ Organic-Based Magnets

Jack G. DaSilva, Amber C. McConnell,[†] and Joel S. Miller*

Department of Chemistry, University of Utah, 315 South 1400 East, Salt Lake City, Utah 84112-0850, United States

ABSTRACT: The pressure dependence of the magnetic properties of ferrimagnetic $Mn^{II}(TCNE)I(OH_2)$ up to 14.05 kbar and $Mn^{II}(TCNE)_{3/2}(I_3)_{1/2}\cdot zTHF$ up to 14.32 kbar were studied. For $Mn^{II}(TCNE)I(OH_2)$, two distinct pressure regions separated at ~1 kbar were evident in both the temperature and the field-dependent magnetic measurements. No increase of the magnetic properties was observed in the low-pressure region, while significant increases to the magnetic ordering temperature, T_c, bifurcation temperature, T_b, coercive field, H_{cr}, and remnant magnetization, M_r, were evident in the high-pressure region. The T_c, T_b, H_{cr}, M_r, and M(5 T) reversibly increased from ambient pressure values of 169 K, 169 K, 690 Oe, 620 emuOe/mol, and 13 800 emuOe/mol to 257 K, 261 K, 1460 Oe, 2300 emuOe/mol, and 17 100 emuOe/mol at 14.05 kbar, respectively. For $Mn^{II}(TCNE)_{3/2}(I_3)_{1/2}\cdot zTHF$, the T_c and T_b were nearly coincident and increased linearly from 173 and 173 K, respectively, at ambient pressure to 273 and 272 K, respectively, at 14.32 kbar. Thus, the T_c increased at an average rate of 6.25 and 7.18 K/kbar for $Mn^{II}(TCNE)I(OH_2)$ and $Mn^{II}(TCNE)_{3/2}(I_3)_{1/2}\cdot zTHF$, respectively. For $Mn(TCNE)_{1/2}(I_3)_{1/2}\cdot zTHF$ remnant magnetization and saturation magnetization did not significantly change with applied pressure. The H_{cr} exhibited a linear increase from ambient pressure to 5.00 kbar, reaching 860 Oe, but only achieving 880 Oe at 14.32 kbar.

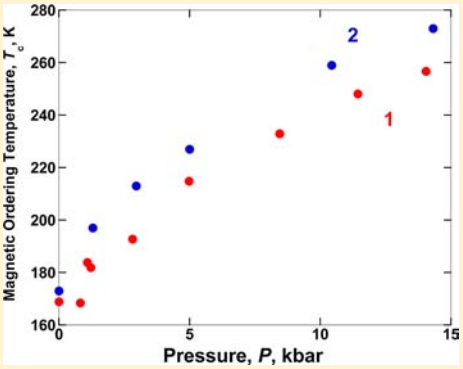

INTRODUCTION

In recent years, much research has centered on the discovery and manipulation of organic-based analogues of metallic and metalloid functional materials.[1] Organic-based magnets (OBM) have advantages over traditional metal and metal oxide magnets.[2−5] OBMs frequently also exhibit photo[6] and piezo active properties.[7] Several OBMs have been synthesized containing $[TCNE]^{\bullet-}$ (TCNE = tetracyanoethylene) including $V(TCNE)_x$, which has a critical temperature (T_c) as high as 400 K.[2−5,8] The inability to structurally resolve this amorphous room temperature OBM has served to fuel the synthesis and structural determination of TCNE containing OBMs.

$M^{II}(TCNE)[C_4(CN)_8]_{1/2}\cdot zCH_2Cl_2$ (M = Fe,[9] Mn[10]) and $[Fe^{II}(TCNE)(NCMe)_2][Fe^{III}Cl_4]$[11] have provided insight into the possible structural features for the high T_c TCNE-containing magnets.[8] The former M = Fe and Mn isostructural compounds possess 3-D connectivity, and all three compounds contain μ_4-$[TCNE]^{\bullet-}$ bound to four M^{II} ions forming corrugated layers. The layers of $M^{II}(TCNE)[C_4(CN)_8]_{1/2}\cdot zCH_2Cl_2$ are connected by diamagnetic $[C_4(CN)_8]^{2-}$ with an average layer separation of 8.71 and 8.77 Å for M = Fe and Mn, respectively. This results in antiferromagnetic ordering with a T_c at ambient pressure of 84 and 69 K for M = Fe and Mn, respectively. $[Fe^{II}(TCNE)(NCMe)_2][Fe^{III}Cl_4]$ consists of 2-D layers with no interlayer connectivity, but has an 8.24 Å interlayer separation, and magnetically orders as a ferrimagnet below 90 K at ambient pressure.[11] $Mn^{II}(TCNE)I(OH_2)$,[12] **1**, and $Mn^{II}(TCNE)_{3/2}(I_3)_{1/2}\cdot zTHF$,[10] **2**, extend this family of structurally related $[TCNE]^{\bullet-}$ containing compounds.

$Mn^{II}(TCNE)_{3/2}(I_3)_{1/2}\cdot zTHF$, **2**, consists of layers separated by 7.96 Å that are interconnected by μ_4-$[TCNE]^{\bullet-}$, Figure 1, which results in ordering as a 3-D ferrimagnet with a T_c and T_b at ambient pressure of 171 and 171 K, respectively.[10] **1** likewise possesses Mn^{II} ions bonded to four μ_4-$[TCNE]^{\bullet-}$ forming 2-D layers, but does not display interconnectivity between layers. The axial positions of the Mn^{II} ions are capped by I^- and H_2O preventing 3-D connectivity and limiting the network structure to 2-D layers, Figure 2.[12] Although $Mn^{II}(TCNE)I(OH_2)$ is 2-D, the interlayer separation is smaller than the other structurally related compounds at 5.00 Å, which yields a correspondingly large T_c of 171 K,[12] similar to the 3-D analogue $Mn^{II}(TCNE)_{3/2}(I_3)_{1/2}\cdot zTHF$.[10]

Detailed magnetic measurements under hydrostatically applied pressure have previously been performed on $Mn^{II}(TCNE)[C_4(CN)_8]_{1/2}\cdot zCH_2Cl_2$,[13] and preliminary magnetic measurements were reported for $Mn^{II}(TCNE)_{3/2}(I_3)_{1/2}\cdot zTHF$.[12] $Mn^{II}(TCNE)[C_4(CN)_8]_{1/2}\cdot zCH_2Cl_2$ exhibited a magnetic transition from antiferromagnetic to ferrimagnetic behavior at 0.50 kbar, which resulted in an initial decrease in the T_c from 69 to ~20 K,

Received: January 31, 2013
Published: March 28, 2013

   dx.doi.org/10.1021/ic400250n | *Inorg. Chem.* 2013, 52, 4629−4634

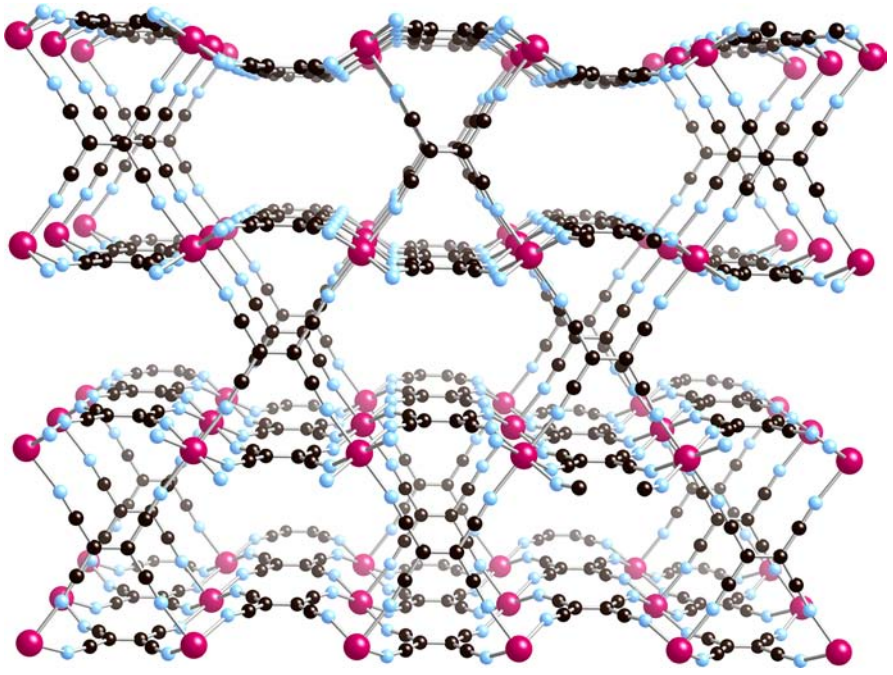

Figure 1. Extended network bonding via μ_4-[TCNE]$^{\bullet-}$ in 3-D present for $Mn^{II}(TCNE)_{3/2}(I_3)_{1/2}$·zTHF (Mn = maroon, C = black, N = blue).[10] The disordered solvent and ordered I_3^- anion reside in the channels.

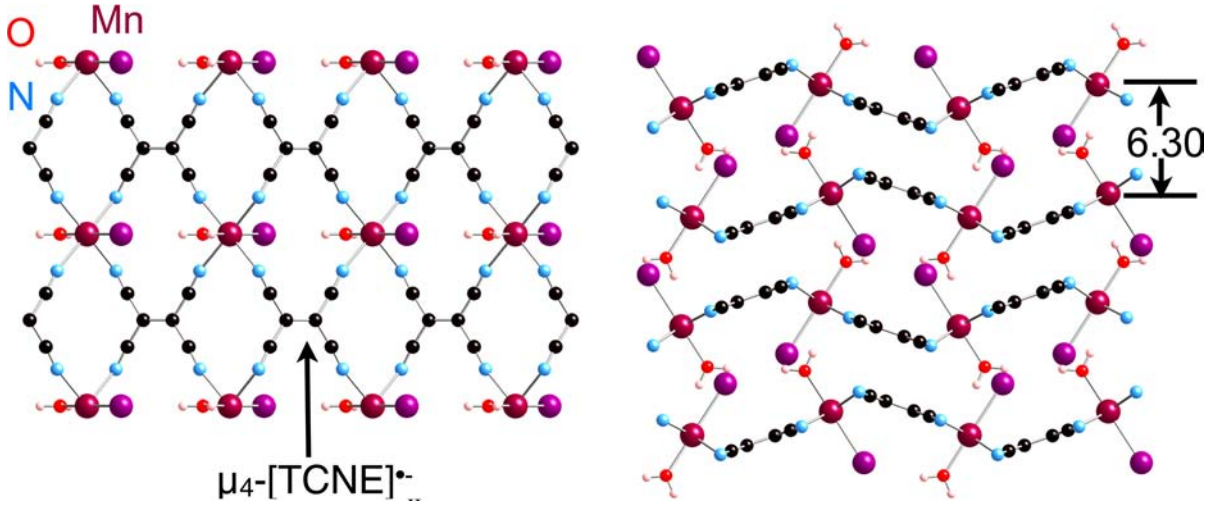

Figure 2. Single layer of the $Mn^{II}(TCNE)I(OH_2)$ structure (left). Side view of multiple layers of the structure of $Mn^{II}(TCNE)I(OH_2)$ (Mn = maroon, C = black, N = blue, O = red, I = purple, H = white) (right).[12]

followed by an increase to ~97 K at 12.6 kbar.[13] There is no hysteresis at ambient pressure; however, an onset was observed above 3.88 kbar, with the coercive field, H_{cr}, increasing with increased pressure, reaching a maximum of 280 Oe.[13] While the ambient pressure magnetic behaviors of these structurally related TCNE-based OBMs are similar [suggesting structural features of $V(TCNE)_x$], the pressure-dependent magnetic behavior was evidence of the subtle structural dependence of magnetic characteristics. The 2- and 3-D structural motifs and resulting magnetic properties have prompted the investigation of the pressure-dependent magnetic behavior of **1** and **2**, and to compare these results with that observed for other materials.

■ EXPERIMENTAL SECTION

$Mn^{II}(TCNE)I(OH_2)$ (**1**)[12] and $Mn^{II}(TCNE)_{3/2}(I_3)_{1/2}$·zTHF (**2**)[10] were prepared similar to those previously described. **1** was prepared in a glovebox under N_2 atmosphere via the dropwise addition of a filtered solution of 35.6 mg of TCNE (0.278 mmol) to 145.8 mg of $MnI_2(THF)_3$ (0.286 mmol) in CH_2Cl_2. The latter solution had 6 mg of distilled H_2O added to it, and it was stirred for 1 h before it was added to the TCNE solution. This reaction was stirred for 10 days. The resulting precipitate was collected by vacuum filtration. **2** was prepared by the above route, using 50.3 mg of TCNE (0.393 mmol) added to 198.3 mg of $MnI_2(THF)_3$ (0.390 mmol), except that water was not added.

Infrared spectroscopy (IR) and AC susceptibility measurements were used to confirm purity, as low-temperature magnetic phases exist for each compound that have similar empirical formulas due to the limited degrees of freedom in the preparation method. The IR spectra were measured from 400 to 4000 cm^{-1} on a Bruker Tensor 37 spectrometer (±1 cm^{-1}) as KBr pellets. A Quantum Design (QD) Physical Property Measurement System, PPMS 9 T, was used to perform AC susceptibility measurements as previously described.[14] Samples of **1** and **2** (3−15 mg) were loaded into gelatin capsules, to

dx.doi.org/10.1021/ic400250n | Inorg. Chem. 2013, 52, 4629−4634

which 10−15 mg of decalin that freezes in the temperature range of the $M(H)$ measurements was added, in an inert atmosphere glovebox and sealed with silicone grease prior to measurement. A QD Superconducting Quantum Interference Device (SQUID) Magnetic Property Measurement System (MPMS-5XL 5 T) (sensitivity = 10^{-8} emu or 10^{-12} emu/Oe at 1 T) was used to perform the pressure-dependent measurements. Samples of **1** (∼1 mg) were loaded into a Teflon cell with ∼1 mg tin (Mallinckrodt, 99.9769%), while samples of **2** were loaded with ∼1 mg of Pb.[15] The remaining volume of the Teflon cell was filled with decalin (the hydrostatic pressure media) that is frozen at the temperatures utilized for $M(H)$ measurements, and capped with Teflon plugs. The Teflon sample cell was placed in a Be−Cu hydrostatic pressure cell based on the Kyowa Seisakusho design with zirconia pistons and rubber o-rings. Pressure was applied to the assemblage using a Kyowa Seisakusho CR-PSC-KY05-1 apparatus and a WG-KY03-3 pressure sensor. An Aikoh Engineering Model-0218B digital sensor readout was used as an approximate pressure guide during pressure application. The applied pressure was determined in situ by measuring the superconducting critical temperature, T_{sc}, of Sn[16a] for **1** and Pb[16b] for **2**, which have a known dependency of T_{sc} as a function of pressure. The estimated error for the pressure is ±0.05 kbar.

The zero-field cooled, $M_{ZFC}(T)$, and field cooled, $M_{FC}(T)$, magnetizations were measured in a 5 Oe applied magnetic field; the $M_{FC}(T)$ and remnant magnetization, $M_r(T)$, were cooled in a 5 Oe applied magnetic field. The T_c was determined as the temperature intercept of the extrapolation of the most linear portion of the remnant magnetization, $M_r(T)$. The bifurcation temperature, T_b, was taken to be the divergence of zero-field cooled, $M_{ZFC}(T)$, and field cooled, $M_{FC}(T)$, magnetizations. Isothermal field-dependent measurements, $M(H)$, were performed at 4 K due to the inclusion of Sn (T_{sc} = 3.732 K).[16] The coercive field, H_{cr}, was determined from the extrapolation of the field intercept at zero magnetization upon reduction from an applied field of ±50 kOe, the remnant magnetization, M_r, was determined from the extrapolation of the magnetization intercept at zero applied field upon reduction of an applied field of ±50 kOe, and the saturation magnetization, M_s, was determined as the magnetization achieved at 5 T applied field.

DISCUSSION

Prior to investigation of the pressure dependence of the magnetic properties of $Mn^{II}(TCNE)I(OH_2)$, **1**, the ambient pressure data were remeasured at 4 K for comparison to the literature values. The T_c and T_b were previously determined to be 171 and 172 K, from the $M_r(T)$ and the $M_{ZFC}(T)$ and $M_{FC}(T)$, respectively.[12] The H_{cr}, M_r, and M(9 T) were previously reported to be 400 Oe, 60 emuOe/mol, and 12 200 emuOe/mol at 5 K.[12] The immiscibility of water and CH_2Cl_2 makes it challenging to replicate reactions and isolate a pure product. This is illustrated by the previously published AC susceptibility, which displays two separate features at lower temperatures in addition to the major peak at 170 K.[12] The ambient pressure T_c, T_b, H_{cr}, and M_r of the sample used for pressure studies were 169 K, 169 K, 690 Oe, and 620 emuOe/mol, respectively. Because of instrumental limitations, the maximum applied field was ±50 kOe, which was insufficient to saturate the magnetization of $Mn^{II}(TCNE)I(OH_2)$. The maximum observed magnetization was 13 800 emuOe/mol at 5 T. The T_c and T_b agreed within the error of the measurements, while the H_{cr}, M_r, and M(5 T) were significantly greater. This is attributed to the lower temperature of the measurement that has led to a larger H_{cr} in several related compounds.[17] In addition, isolation of a purer sample of $Mn^{II}(TCNE)I(OH_2)$ than has previously been measured could also be expected to yield a larger H_{cr}. Likewise, M_r and M(5 T) have been found to depend on purity and crystal alignment in some materials.[18,19]

The pressure dependence of $M_{ZFC}(T,P)$, $M_{FC}(T,P)$, and $M_r(T,P)$ had virtually no change below ∼1 kbar for **1**, but both T_b and T_c increase with increasing pressure above 1 kbar, Figure 3. Above ∼1 kbar, the T_c and T_b increase approximately

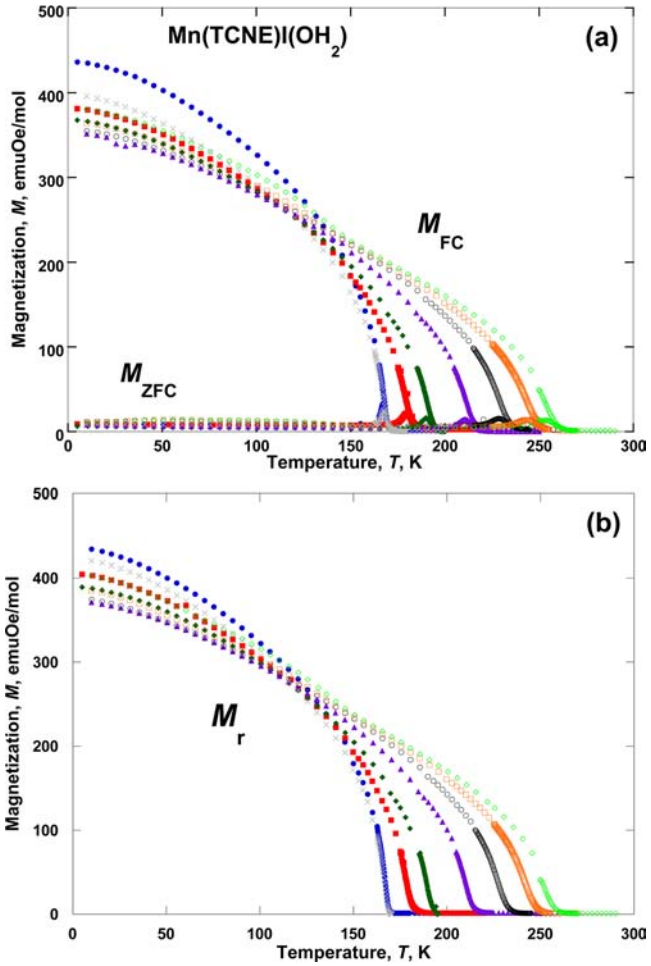

Figure 3. Pressure dependence of the $M_{ZFC}(T)$ and $M_{FC}(T)$ (a) and the $M_r(T)$ (b) for **1**: 0.82 (●), 1.22 (■), 2.82 (◆), 4.98 (▲), 8.45 (○), 11.44 (□), 14.05 kbar (◇), and upon returning to approximately ambient pressure [0.52 kbar (×)] for $Mn^{II}(TCNE)I(OH_2)$.

linearly to 257 and 261 K at the maximum applied pressure of 14.05 kbar, at an average rate of 6.25 and 6.58 K/kbar, respectively, Figure 4. Upon release of the applied pressure, the T_c and T_b were recovered, indicating reversibility. The decrease of $M_{ZFC}(T,P)$, $M_{FC}(T,P)$, and $M_r(T,P)$ is in agreement with previously reported studies,[15,20] up to 4.98 kbar, above which an anomalous increase in the magnetization was observed, Figure 3. The increase in the magnetization at intermediate to high pressures resembles that observed for $[Ru_2(O_2CMe)_4]_3[Cr(CN)_6]$ above 5.45 kbar,[15] even though it is not as pronounced for $Mn^{II}(TCNE)I(OH_2)$.

At ambient pressure and 4 K, $Mn^{II}(TCNE)I(OH_2)$ has a H_{cr}, of 690 Oe, magnetization at 5 T of 13 800 emuOe/mol, and M_r of 620 emuOe/mol, which are higher than the previously reported values of 400 Oe, 8350 emuOe/mol at 5 T (12 200 emuOe/mol at 9 T), and 60 emuOe/mol, respectively.[12] With increasing pressure, the $M(H,P)$ at 4 K was similar to T_c and T_b with little change below ∼1 kbar, followed by an approximately

dx.doi.org/10.1021/ic400250n | Inorg. Chem. 2013, 52, 4629−4634

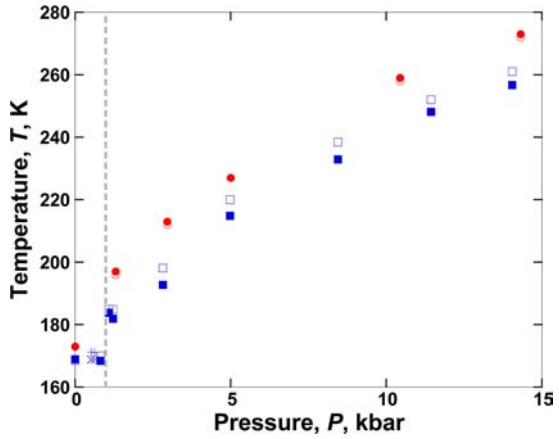

Figure 4. Pressure dependence of T_c (■), T_b (□) for **1** and T_c (●), T_b (○) for **2**; released pressure data are "+" and "×". The dashed line at ∼1 kbar represents the separation of the high- and low-pressure regions for **1**.

linear increase of the H_{cr} and M_r to 1460 Oe and 2300 emuOe/mol at 14.05 kbar, respectively, Figures 5 and 6. The qualitative

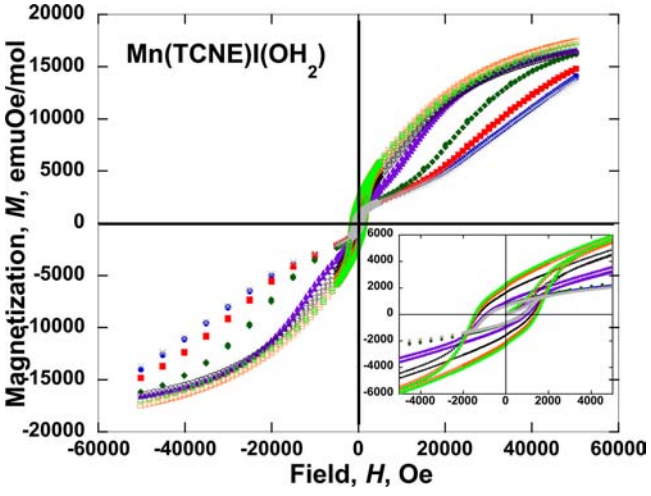

Figure 5. Pressure dependence of the $M(H)$ of **1** at 0.82 (●), 1.22 (■), 2.82 (◆), 4.98 (▲), 8.45 (○), 11.44 (□), 14.05 kbar (◇), and upon returning to approximately ambient pressure [0.52 kbar (×)]. Inset displays the hysteretic loop ±5000 Oe.

shape of the hysteresis loops transitioned between 2.82 and 4.98 kbar, from the complex ambient pressure behavior to a more standard shape, approaching saturation at 5 T instead of ∼8 T, Figure 5, which was previously observed at ambient pressure.[12] The M_s values above 2.82 kbar were as much as 40% greater than the literature value of 12 200 emuOe/mol, reaching 17 400 emuOe/mol at 11.44 kbar. This disparity is likely due in part to the enhanced purity with respect to previous samples (vide supra). Also, the M_s increased by 900 emuOe/mol with an increase of pressure from 4.98 to 11.44 kbar, which suggests that $Mn^{II}(TCNE)I(OH_2)$ does not saturate in ±5 T applied field until ∼11.44 kbar. Upon release of the applied pressure, the H_{cr}, M_r, and M(9 T) were recovered, indicating reversibility. The results are summarized in Table 1.

The ambient pressure magnetic properties of **2** were also reinvestigated prior to measurement of the pressure dependence for comparison to the literature values. The T_c and T_b

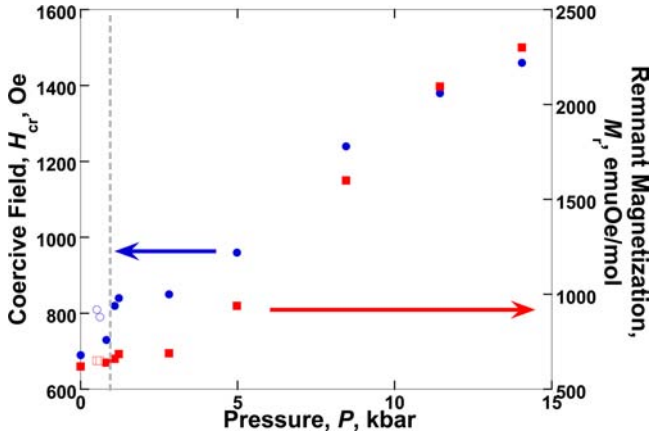

Figure 6. Pressure dependence of H_{cr} (●) and M_r (■) of **1**; released pressure measurements are hollow. The dashed line at approximately 1 kbar represents the separation of the high- and low-pressure regions.

were previously determined to be 171 and 171 K, from the $M_r(T)$ and the $M_{ZFC}(T)$ and $M_{FC}(T)$, respectively.[10] These values were reasonably reproduced with values of 173 and 173 K for the T_c and T_b, respectively. The H_{cr}, M_r, and M_s were previously reported to be 600 Oe, 8000 emuOe/mol, and 21 800 emuOe/mol at 10 K.[10] The field-dependent properties were reproduced with less accuracy at 710 Oe, 5300 emuOe/mol, and 18 200 emuOe/mol for the H_{cr}, M_r, and M_s, respectively. As for **1**, the field-dependent properties of compound **2** appear to be significantly affected by the crystalline quality of a given sample.

The pressure dependence of the $M_{ZFC}(T,P)$, $M_{FC}(T,P)$, and $M_r(T,P)$ increases linearly with increasing pressure, Figure 7. The T_c from the $M_r(T,P)$ and T_b from the $M_{ZFC}(T,P)$ and $M_{FC}(T,P)$ increase to 273 and 272 K at 14.32 kbar (58% and 57%, respectively), Figures 4 and 7. Similar to **1**, the low-temperature $M_{ZFC}(T,P)$, $M_{FC}(T,P)$, and $M_r(T,P)$ magnetizations of **2** decrease with increasing pressure, as has been observed previously;[20] but unlike **1**, it exhibits an anomalous improvement at intermediate pressures, Figure 7. Upon release of the applied pressure, the T_c and T_b were recovered, indicating reversibility. The results are summarized in Table 1.

The M_r and M(5 T) at 10 K decrease slightly with applied pressure, with values of 5300 and 17 000 emuOe/mol at 14.32 kbar, Figure 8. The H_{cr} increased throughout the range of applied pressures, achieving a maximum of 880 Oe, but exhibited a greater rate of increase at low pressures than at high pressures; the division of the high- and low-pressure regions for the H_{cr} increases occurring at ∼5 kbar, Figure 9. The hysteretic behavior and shape remained consistent at all applied pressures, Figure 8. Upon release of the applied pressure, the T_c and T_b were recovered, indicating reversibility.

The 2-D and 3-D structural motifs of **1** and **2** are responsible for the variation of their respective pressure dependencies: **1** exhibited an average rate of change for T_c and T_b of 6.25 and 6.58 K/kbar, respectively, while **2** exhibited rates of 7.18[10] and 7.06 K/kbar, respectively. The average values for **1** are skewed somewhat by the existence of a high- and low-pressure region characterized by distinct rates of enhancement of T_c, T_b, and H_{cr}, Figures 4 and 6. The rate of increase of the T_c and T_b is comparable to that observed for $M^{II}(TCNE)[C_4(CN)_8]_{1/2}\cdot zCH_2Cl_2$ (6.2 and 6.6 K/kbar, respectively),[13] and $Mn^{II}(TCNE)_{3/2}(I_3)_{1/2}\cdot zTHF$ (7.18 and 7.06 K/kbar, respectively).[10] The response of 2-D **1** to pressure was similar

dx.doi.org/10.1021/ic400250n | Inorg. Chem. 2013, 52, 4629−4634

Table 1. Summary of the Ambient and Pressure-Dependent Magnetic Behavior for 1 and 2

	P, kbar	T_c, K	rate,[a] K/kbar	T_b, K	rate,[a] K/kbar	H_{cr}, Oe	M(5 T), emuOe/mol	M_r, emuOe/mol
1	ambient[12]	171		172		400	8350	60
1	ambient	169		169		690	13 800	620
1	14.05	257	6.25	261	6.58	1460	17 100	2300
2	ambient[10]	171		171		600	18 200	8000
2	ambient	173		173		860	18 200	5300
2	14.32	273	7.18[10]	272	7.06	880	17 100	5200

[a] Average.

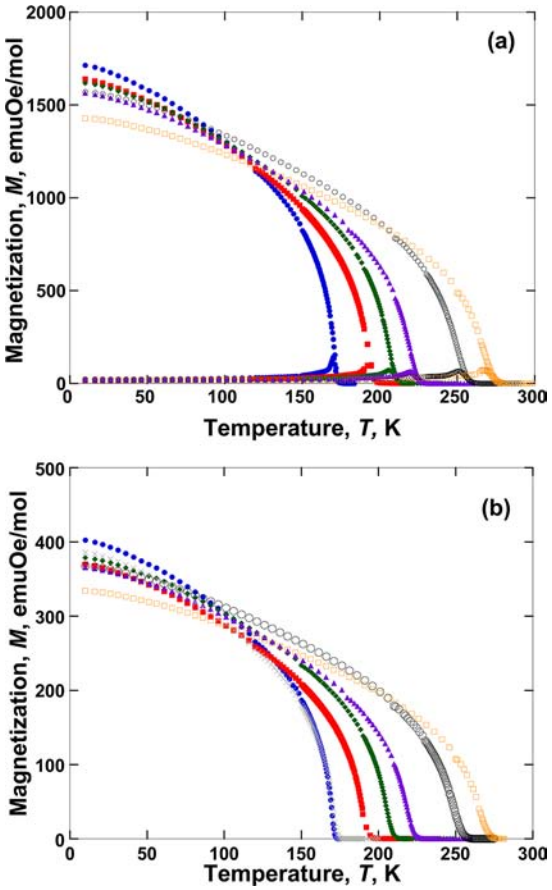

Figure 7. Pressure dependence of the $M_{ZFC}(T)$ and $M_{FC}(T)$ (a) and the $M_r(T)$ (b) for **2**: 0.001 (●), 1.30 (■), 2.96 (◆), 5.00 (▲), 10.44 (○), 14.32 (□), and upon returning to ambient pressure [0.001 kbar (×)] for $M_r(T)$ of **2**.

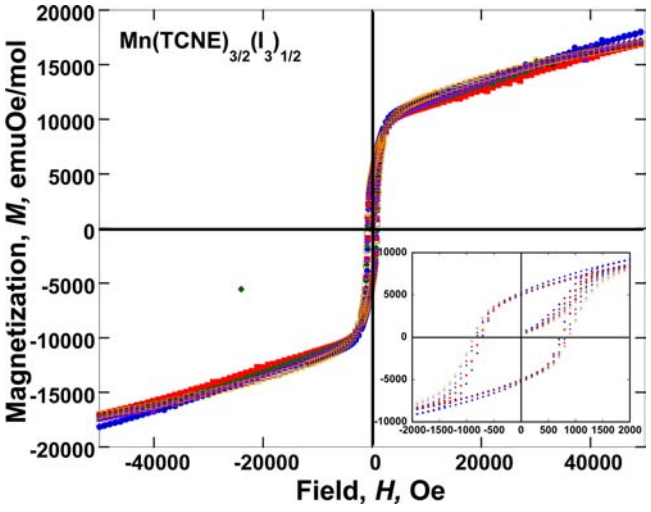

Figure 8. Pressure dependence of the $M(H)$ at 10 K: 0.001 (●), 1.30 (■), 2.96 (◆), 5.00 (▲), 10.44 (○), and 14.32 (□) for **2**. Inset displays the hysteretic loop ±2000 Oe.

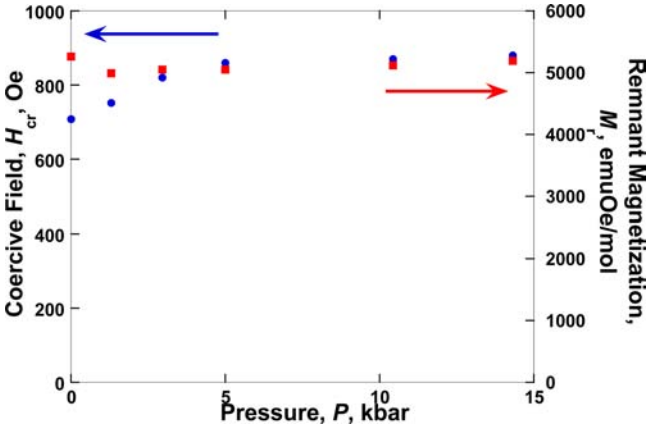

Figure 9. Pressure dependence of H_{cr} (●) and M_r (■) of **2**; released pressure measurements are concurrent with ambient pressure data points.

to the 3-D **2** when only the high-pressure regime was considered, 6.67 and 6.88 K/kbar for the T_c and T_b, respectively, Figure 4. Presumably, these improvements are due to the contraction of interatomic distances, thereby increasing the coupling through increased overlap of the $[TCNE]^{\bullet-}$ π^* and Mn d-orbitals. Interestingly, although $Mn^{II}(TCNE)I(OH_2)$ is composed of 2-D layers, the trends observed in the magnetic data lack the complexity expected of improved interlayer coupling, the suppression of hysteretic behavior. This suggests that the interlayer interaction in $Mn^{II}(TCNE)I(OH_2)$ is either significantly weak, even with reduced interlayer separation, resulting in insufficient coupling to suppress the hysteretic behavior, or that the interaction is of quite a different nature than that expected through space antiferromagnetic coupling. The increased coercivity with applied pressure for **1** is qualitatively similar to that observed for **2** and $M^{II}(TCNE)[C_4(CN)_8]_{1/2}\cdot zCH_2Cl_2$, which increased from zero at ambient pressure to 280 Oe at 12.6 kbar,[13] which further suggests a unique interlayer interaction.

The existence of two distinct pressure regions is presumably due to the 2-D structural motif of $Mn^{II}(TCNE)I(OH_2)$, where the low-pressure region is representative of interlayer compression over a distance insufficient to perturb the magnetic interaction between layers, thus resulting in a lack of significant increase in the T_c, T_b, H_{cr}, or M_r. The similarity of the pressure-induced increase in T_c and T_b for **2** serves as a useful illustration of the macroscopic consequences of 3-D

dx.doi.org/10.1021/ic400250n | Inorg. Chem. 2013, 52, 4629−4634

connectivity. **2** responds immediately and continually to applied pressure in contrast to the 2-D **1**, and, as the most significant structural difference between the two structures is the connectivity, it may be inferred that this quality is responsible for the varied behavior of the compounds.

CONCLUSION

The pressure-dependent magnetic behavior of **1** was measured up to 14.05 kbar, with emphasis around ∼1 kbar, which approximates a transition in the pressure-dependent magnetic behavior, and was measured up to 14.32 kbar for **2**. Both compounds displayed pressure-induced enhancement of magnetic properties. 2-D $Mn^{II}(TCNE)I(OH_2)$ exhibits a high T_c and substantial response to applied pressure up to 14.05 kbar, which more closely resembles the behavior of the related 3-D compounds, **2** and $Mn^{II}(TCNE)[C_4(CN)_8]_{1/2}\cdot zCH_2Cl_2$. This behavior suggests that the initial pressurization reduces the interlayer separation of $Mn^{II}(TCNE)I(OH_2)$. Above ∼1 kbar, the interlayer separation has reduced sufficiently to allow significant or increased interlayer coupling. The nature of this unknown coupling mechanism makes further structural and spectroscopic studies of $Mn^{II}(TCNE)I(OH_2)$ under applied pressure important.

AUTHOR INFORMATION

Corresponding Author

*E-mail: jsmiller@chem.utah.edu.

Present Address

[†]Department of Chemistry, Southern Utah University, Cedar City, Utah 84720, United States.

Notes

The authors declare no competing financial interest.

ACKNOWLEDGMENTS

We appreciate Royce A. Davidson for his assistance with diamagnetic corrections due to the excessive mass of the BeCu pressure apparatus, and the late Joshua D. Bell for preparation of the sample, as well as the continued support by the Department of Energy Division of Material Science (Grant no. DE-FG03-93ER45504).

REFERENCES

(1) Miller, J. S. *Adv. Mater.* **1990**, *2*, 98.
(2) Miller, J. S. *Chem. Soc. Rev.* **2011**, *40*, 3266.
(3) Ovcharenko, V. I.; Sagdeev, R. Z. *Russ. Chem. Rev.* **1999**, *68*, 345.
(4) Blundell, S. J.; Pratt, F. L. *J. Phys.: Condens. Matter* **2004**, *16*, R771.
(5) Miller, J. S.; Epstein, A. J. *Angew. Chem., Int. Ed. Engl.* **1994**, *33*, 385.
(6) Varret, F.; Nogues, M.; Goujon, A. In *Magnetism: Molecules to Materials*; Miller, J. S., Drillon, M., Eds.; Wiley-VCH: New York, 2000; Vol. *1*, p 257.
(7) (a) Rabu, P.; Drillon, M.; Awaga, K.; Fujita, W.; Sekine, T. In *Magnetism: Molecules to Materials*; Miller, J. S., Drillon, D., Eds.; Wiley-VCH: Weinheim, 2001; Vol. *2*, p 357. (b) Nakatsuji, S. *J. Synth. Org. Chem., Jpn.* **2003**, *61*, 670.
(8) Miller, J. S. *Polyhedron* **2009**, *28*, 1596.
(9) Her, J.-H.; Stephens, P. W.; Pokhodnya, K. I.; Bonner, M.; Miller, J. S. *Angew. Chem., Int. Ed.* **2007**, *46*, 1521.
(10) Stone, K. H.; Stephens, P. W.; McConnell, A. C.; Shurdha, E.; Pokhodnya, K. I.; Miller, J. S. *Adv. Mater.* **2010**, *22*, 2514.
(11) Pokhodnya, K. I.; Bonner, M.; Her, J.-H.; Stephens, P. W.; Miller, J. S. *J. Am. Chem. Soc.* **2006**, *128*, 15592.
(12) Lapidus, S. H.; McConnell, A. C.; Stephens, P. W.; Miller, J. S. *Chem. Commun.* **2011**, *47*, 7602.
(13) McConnell, A. C.; Bell, J. D.; Miller, J. S. *Inorg. Chem.* **2012**, *51*, 9978.
(14) Kareis, C. M.; Her, J.-H.; Stephens, P. W.; Moore, J. G.; Miller, J. S. *Chem.-Eur. J.* **2012**, *18*, 9281. Brandon, E. J.; Rittenberg, D. K.; Arif, A. M.; Miller, J. S. *Inorg. Chem.* **1998**, *37*, 3376.
(15) Shum, W. W.; Her, J.-H.; Stephens, P. W.; Lee, Y.; Miller, J. S. *Adv. Mater.* **2007**, *19*, 2910.
(16) (a) Jennings, L. D.; Swenson, C. A. *Phys. Rev.* **1958**, *112*, 31. (b) Clark, M. J.; Smith, T. F. *J. Low Temp. Phys.* **1978**, *32*, 495.
(17) (a) Chittipeddi, S.; Cromack, K. R.; Miller, J. S.; Epstein, A. J. *Phys. Rev. Lett.* **1987**, *58*, 2695. (b) Rittenberg, D. K.; Sugiura, K.-i.; Sakata, Y.; Mikami, S.; Epstein, A. J.; Miller, J. S. *Adv. Mater.* **2000**, *12*, 126. (c) Sun, H.-L.; Wang, Z.-M.; Gao, S. *Chem.-Eur. J.* **2009**, *15*, 1757. (d) Sessoli, R. *Angew. Chem., Int. Ed.* **2008**, *47*, 5508. (e) Ishii, N.; Okamura, Y.; Chiba, S.; Nogami, T.; Ishida, T. *J. Am. Chem. Soc.* **2008**, *130*, 24.
(18) Taliaferro, M. L.; Palacio, F.; Miller, J. S. *J. Mater. Chem.* **2006**, *16*, 2677.
(19) Morrish, A. H. *The Physical Principles of Magnetism*; John Wiley & Sons, Inc.: New York, 1965; pp 340−60.
(20) DaSilva, J. G.; Miller, J. S. *Inorg. Chem.* **2013**, *52*, 1108.